Journal of Catalysis **210,** 46–52 (2002)
doi:10.1006/jcat.2002.3680

The Role of Lattice Oxygen in Selective Benzyl Alcohol Oxidation Using OMS-2 Catalyst: A Kinetic and Isotope-Labeling Study

Vinit D. Makwana,* Young-Chan Son,* Amy R. Howell,* and Steven L. Suib*,†,‡,[1]

*Department of Chemistry, †Department of Chemical Engineering, and ‡Institute of Material Sciences, U-3060, University of Connecticut, Storrs, Connecticut 06269

Received November 21, 2001; revised May 14, 2002; accepted May 20, 2002

The oxidation of benzyl alcohol by molecular O_2 in the liquid phase using a heterogeneous octahedral molecular sieve (OMS) catalyst was studied. Typical batch reactor kinetic data were obtained and fitted to the classical Langmuir–Hinshelwood–Hougen–Watson (LHHW) model as well as to the Mars–van Krevelen (MvK) model of heterogeneously catalyzed reactions. A two-step Mars–van Krevelen model involving an exchange between the gas phase and lattice oxygen was found to give a better fit. This was further corroborated by an oxygen-isotope-labeling study. The changes in the ^{16}O and ^{18}O content of the product water confirm this observation. Kinetic isotope effects were also evaluated in mechanistic studies. The occurrence of this mechanism in the liquid phase explains the activity and high selectivity of the OMS-2 catalyst for this selective oxidation reaction.

Key Words: **octahedral molecular sieves (OMS); alcohol oxidation, Mars–van Krevelen mechanism.**

INTRODUCTION

Oxidation is one of the most important process steps for producing fine chemicals from petroleum and vegetable feedstocks. Selective oxidation of the hydroxyl group of alcohols is the most common of oxidations, and a variety of techniques for carrying this out are known. Alcohol oxidation is conventionally performed with stoichiometric amounts of Cr(VI) compounds or other inorganic oxidants (1). The major drawback of this stoichiometric protocol is the generation of large amounts of heavy metal waste. This gives rise to the need for milder catalytic processes utilizing dioxygen or H_2O_2 as the oxygen source (2–4). Due to the handling hazards associated with peroxides, and its usual availability as an aqueous solution, molecular oxygen is preferred as an environmentally acceptable, selective, strong oxidant for liquid-phase oxidations (5).

Most of the processes designed to use O_2 as an oxidant are based on the radical chain autooxidation reaction. The controlling step in such reactions is the formation of unstable peroxides by the reaction of dioxygen with free radicals. The high reactivity of radical intermediates gives a mixture of products, and high selectivity is difficult to achieve. Another catalytic oxygen activation procedure is to use a metal catalyst and an oxygen donor to form an oxometal or a peroxometal intermediate. In the peroxometal route, the oxidation state of the metal ion remains unchanged and the metal ion simply acts as a Lewis acid, increasing the oxidizing power of the peroxo group. The oxometal pathway, on the other hand, involves a two-electron reduction of the metal ion, which is subsequently reoxidized by the oxygen donor. This latter pathway is known as the Mars–van Krevelen mechanism (6) and is observed in gas-phase oxidations more commonly than in liquid phase (7).

Apart from the oxidation of benzene and naphthalene in Mars' and van Krevelen's original paper, some recent examples of this mechanism are the oxidation of allyl iodide (8) to acrolein and of *n*-butane to maleic anhydride (9). The only reported liquid-phase Mars–van Krevelen-mechanism-type oxidation uses a homogeneous phosphovanadomolybdate catalyst (10). We recently reported a method to catalytically oxidize alcohols in the liquid phase, using a MnO_x catalyst and molecular oxygen in air as the oxidant (11). Results of this study suggest that the above heterogeneous oxidation occurs via a Mars–van Krevelen mechanism in the liquid phase.

EXPERIMENTAL

Reagents

All reagents used were of analytical grade, unless otherwise noted. The air used as an oxygen source was supplied by a utility compressor and used as such without any further treatment.

Catalyst Preparation

The catalyst used for the present study (cryptomelane) belongs to a class of synthetic manganese oxide materials with a tunnel structure, called octahedral molecular sieves (OMS) (12, 13). Synthetic cryptomelane has a one-dimensional tunnel structure formed by 2×2 edge shared

[1] To whom correspondence should be addressed. Fax: 1-860-486-2981. E-mail: suib@uconnvm.uconn.edu.

0021-9517/02 $35.00

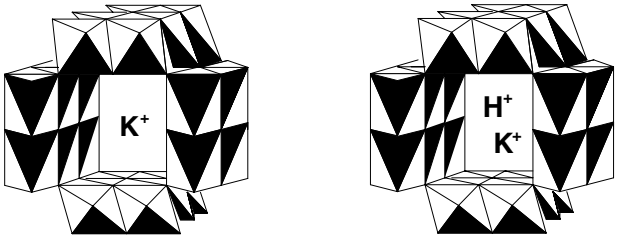

FIG. 1. Structure of K–OMS-2 and H–K–OMS-2 catalysts.

MnO_6 octahedral chains and is commonly called OMS-2. The tunnels have dimensions of 4.6 × 4.6 Å, while the overall composition is $KMn_8O_{16} \cdot nH_2O$ (Fig. 1).

OMS-2 was prepared by the precipitation method (14). A 0.4 M solution of $KMnO_4$ (13.3 g in 225 mL of distilled, deionized water) was added to a mixture of a 1.75 M solution of $MnSO_4 \cdot H_2O$ (19.8 g in 67.5 mL of DDW) and 6.8 mL of concentrated HNO_3. The resulting black precipitate was stirred vigorously and refluxed at 373 K for 24 h. The precipitate was filtered and washed with DDW until neutral pH and dried overnight at 393 K. This gave the K^+ form of OMS-2.

The K–OMS-2 was doped with H^+ to form the H–K–OMS-2 catalyst. K–OMS-2 (2.5 g) was added to 50 mL of 1 M HNO_3 and the mixture was stirred vigorously at ∼333–343 K for 3–20 h. After a similar washing and drying procedure, an elemental analysis of the final product revealed a 20% ion exchange, giving the final composition of the H–K–OMS-2 catalyst as $H_{0.2}K_{0.8}Mn_8O_{16} \cdot nH_2O$.

Surface Area Measurements

The surface areas of both K–OMS-2 and H–K–OMS-2 were measured by the Brunauer–Emmett–Teller (BET) method on a Micromeritics ASAP 2010 instrument. The measurements were made using N_2 gas as the adsorbent and with a multipoint method. The surface area of K–OMS-2 was found to be ∼97 $m^2\ g^{-1}$, while that of H–K–OMS-2 was found to be ∼85 $m^2\ g^{-1}$.

X-Ray Powder Diffraction Studies

Both the K–OMS-2 and the H–K–OMS-2 catalysts were characterized by XRD methods. Data were collected using a Scintag 2000 PDS instrument with Cu $K\alpha$ radiation with a beam voltage of 45 kV and a 40-mA beam current. The structure was verified by comparing with standards and was conserved even after ion exchange.

Experimental Procedure

In a typical kinetic experiment, 15 mL of toluene (J. T. Baker), 1 mmol of the substrate alcohol (benzyl alcohol, Janssen Chimica), and 0.5 mmol of methyl benzoate (Aldrich) as an internal standard were put in a three-neck round-bottomed flask. The catalyst (∼50 mg (0.5 eq), considering one manganese atom to be one active site) was added and a reflux condenser was attached. One of the remaining ports served as an inlet for the air sparger, while the third served as a sampling port. This assembly was placed in a paraffin oil bath. Air was bubbled at a high flow rate of ∼200 mL/min and the reaction mixture was vigorously stirred. The reaction was thus carried out under semibatch conditions for 4 h. The reflux conditions ensured a constant temperature equal to the b.p. of toluene (383 K). Samples of the reaction mixture (∼0.1 ml) were withdrawn by microsyringe at regular intervals of time. The microsyringe was fitted with a 0.5-μm inline filter to exclude the solid catalyst particles.

Analytical Procedure

Gas chromatography–mass spectrometry (GC–MS) methods were used for the identification and quantification of product mixtures. The GC–MS analyses were done using a HP 5890 series II chromatograph with a thermal conductivity detector coupled with a HP 5970 mass selective detector. The column used was a HP-1 (cross-linked methyl siloxane) with dimensions of 12.5 m × 0.2 m × 0.33 μm.

Isotope Labeling Experiments

Experimental evidence of the Mars–van Krevelen mechanism was sought by oxygen isotope labeling. The oxidation of benzyl alcohol on H–K–OMS-2 with $^{18}O_2$ was followed in time at a constant reaction temperature of 383 K. The same reactor setup and reaction mixture as in the kinetic experiment was used, with the only difference being that a smaller quantity (0.1 eq) of catalyst was added. The reactor was connected downstream to an online mass spectrometer (MKS Instruments) via a continuous-leak valve. The MS can be used to make continuous scans for set m/z values. The reactor assembly was loaded with the reaction mixture and purged with a 20% mixture of $^{18}O_2$ (99%, Icon Isotopes) in He (UHP, Airgas) at room temperature for 120 min. This pretreatment procedure ensured almost complete removal of atmospheric and dissolved $^{16}O_2$. However, this room temperature treatment is not enough to replace the chemisorbed $^{16}O_2$ on the catalyst. The reactor was heated to 383 K and the reaction was carried out for 80 min. The products $H_2{}^{16}O$ and $H_2{}^{18}O$ were detected with the mass spectrometer.

The exchange of oxygen without participation of a redox mechanism was also studied. A glass tubular reactor loaded with 30 mg of the K–OMS-2 catalyst was placed in a tubular furnace and purged with He (UHP, Airgas) for 2 h at a reaction temperature of 110°C. After this pretreatment, a 20% mixture of $^{18}O_2$ (99%, Icon isotopes) in He was passed over the catalyst at the same temperature for 70 min. The exhaust stream was monitored online with a mass spectrometer for $H_2{}^{18}O$.

Kinetic Isotope Labeling

The kinetic isotope effect ratio (k_H/k_D) was found by determining k_H and k_D separately under pseudo-first-order reaction conditions. The same experimental procedure was used involving 1 mmol of benzyl alcohol, 3 eq of H–K–OMS-2, and 0.5 mmol of methyl benzoate as the internal standard in toluene. The large excess of catalyst and a high flow rate of air with intense stirring ensured pseudo-first-order conditions. Samples were removed at regular intervals of time with microsyringes fitted with inline microfilters to exclude catalyst particles. The same procedure was repeated with α,α-dideuteriobenzyl alcohol (98 atom% D, Aldrich) instead of benzyl alcohol to obtain k_D.

Acidity Measurements

In situ IR spectra of pyridine adsorbed on the catalysts were used to determine the type and number of acidic sites on the catalyst. A 10- to 20-mg self-supported sample wafer of OMS-2 in KBr was dehydrated at 400°C under a vacuum of $\sim 10^{-4}$ Torr for 3 h. A blank spectrum was recorded at room temperature on a Nicolet Magna-IR Spectrometer 750. The sample holder was remounted on the vacuum line without loss of vacuum and the sample was exposed to pyridine vapors at room temperature for 30 min, followed by desorption for 30 min, also at room temperature, before the IR spectra were recorded.

RESULTS

Effect of Mass Transfer

The process is a typical slurry-phase reaction with one liquid reactant, a solid catalyst, and one gaseous reactant. As with any multiphase reaction, mass transfer effects are likely to mask the true kinetics of this reaction. Hence, before investigating any oxidation kinetics, we first need to eliminate any mass transfer limitations that might exist. Figure 2 shows the effect of speed of agitation on conversion. The abscissa denotes stirring speeds while the Y-axis shows conversion after 4 h of reaction. As seen in the figure, conversion initially increases with stirring, denoting a mass-transfer-controlled regime. The latter part of the graph shows conversion to be independent of stirring, indicating a kinetic control regime. This is our region of interest and all further experiments were done at a stirrer setting of 1800 rpm or higher.

Oxidation of Benzyl Alcohol in Toluene

A plot of benzyl alcohol conversion (X) vs time on K–OMS-2 and H–K–OMS-2 catalysts is shown (Fig. 3). The derivative at any point on these curves gives the rate. The design equation for an isothermal, well-mixed batch reactor

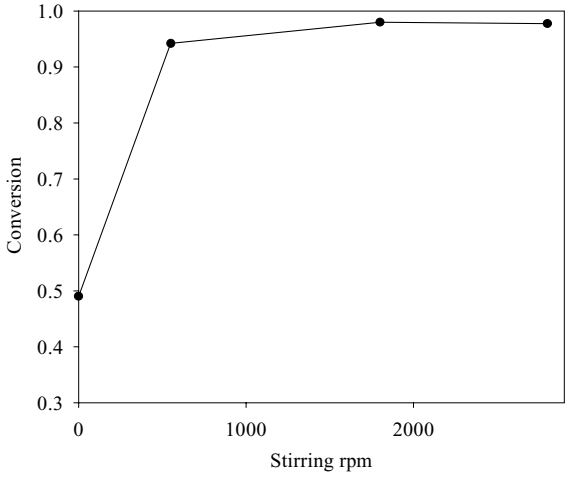

FIG. 2. Effect of mass transfer on alcohol oxidation.

is (15)

$$\text{rate} = -dC/dt, \qquad [1]$$

where C is the concentration of the reactant at time t. As seen from these curves, the partial substitution of K^+ by H^+ has a positive effect on conversion.

Reaction Kinetics Analysis

The kinetics of the reaction can be expressed as a power law rate,

$$\text{Rate} = k[\text{PhCH}_2\text{OH}]^a[\text{O}_2]^b, \qquad [2]$$

where k is the rate constant and a and b are the reaction orders with respect to benzyl alcohol and oxygen, respectively. However, such a representation has limited utility for mechanistic elucidation. Hence, we have followed the approach of fitting experimental kinetic data to one of the

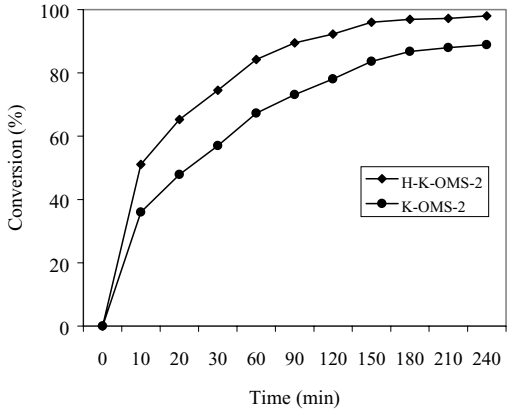

FIG. 3. Conversion vs time for benzyl alcohol over different catalysts. Selectivity to aldehyde for both runs, 100%.

three possible mechanisms of heterogeneous catalysis:

(i) the Eley–Rideal mechanism;
(ii) the Langmuir–Hinshelwood–Hougen–Watson mechanism (LHHW); or
(iii) the Mars–van Krevelen mechanism.

The Eley–Rideal mechanism requires one of the reactants to be in the gas phase. However, here the reacting species is dissolved oxygen, and hence this mechanism is not applicable. The LHHW rate equation finds frequent application for correlating heterogeneous catalysis kinetics. This mechanism involves adsorption of the reacting species (benzyl alcohol and oxygen) on active sites at the surface, followed by an irreversible, rate-determining surface reaction to give products. The LHHW rate law can be derived from the above elementary steps as

$$\text{Rate} = \frac{kK_1K_2^{0.5}[\text{PhCH}_2\text{OH}][\text{O}_2]^{0.5}}{[1 + K_1[\text{PhCH}_2\text{OH}] + K_2^{0.5}[\text{O}_2]^{0.5}]^2} \qquad [3]$$

where k is the rate constant for the surface reaction and K_1 and K_2 are the adsorption desorption equilibrium constants for $PhCH_2OH$ and O_2, respectively. Conversion is invariant whether air is bubbled through the slurry phase or just passed over the liquid surface. This implies that mass transfer of oxygen to the liquid phase is not rate controlling and the dissolved O_2 concentration is constant. Equation [3] can be transformed by lumping together all the constants to yield

$$\text{Rate} = \frac{a[\text{PhCH}_2\text{OH}]}{[b + c[\text{PhCH}_2\text{OH}]]^2}. \qquad [4]$$

We used a nonlinear regression analysis to fit the experimental data to Eq. [4] after converting the concentration variable to the conversion variable. Figure 4 shows the model fit as compared to actual experimental data. The sum of residuals is 0.63.

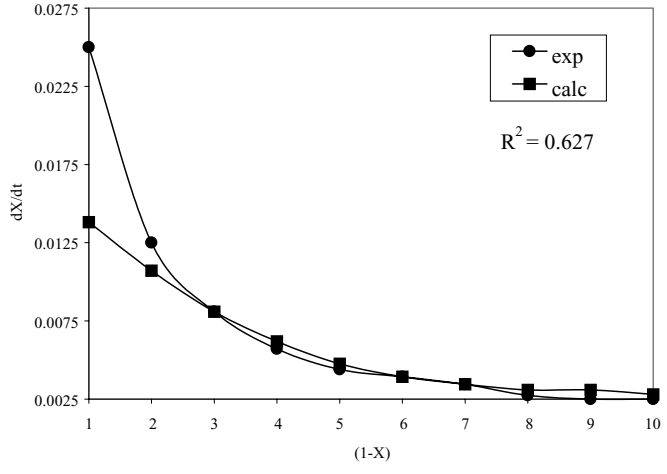

FIG. 4. Langmuir–Hinshelwood–Hougen–Watson kinetic model fitting.

The Mars–van Krevelen mechanism, though first proposed in 1954, has recently gained wide application for explaining selective oxidation over transition metal oxides. The mechanism comprises two reaction steps. In the first step, the lattice oxygen oxidizes the substrate molecule, followed by a reoxidation of the partially reduced catalyst by molecular oxygen. The rate of oxidation of the substrate can be expressed as

$$\text{Rate}_1 = k_1[\text{PhCH}_2\text{OH}]\theta, \qquad [5]$$

where θ = degree of catalyst surface occupied by the substrate.

The rate of reoxidation of the surface is proportional to the surface not covered by oxygen and can be expressed as

$$\text{Rate}_2 = k_2[\text{O}_2]^n(1 - \theta). \qquad [6]$$

At steady state, both these rates would be equal, hence

$$\beta k_1[\text{PhCH}_2\text{OH}]\theta = k_2[\text{O}_2]^n(1 - \theta), \qquad [7]$$

where $\beta = 0.5$, the stoichiometric coefficient for O_2.

Eliminating θ from Eq. [7] and substituting in Eq. [5], we get the final rate expression for the Mars–van Krevelen mechanism,

$$\text{Rate} = \frac{1}{\frac{1}{k_1[\text{PhCH}_2\text{OH}]} + \frac{0.5}{k_2[\text{O}_2]^n}}, \qquad [8]$$

where k_1 and k_2 are rate constants for the two reaction steps, respectively. Substituting $[O_2]$ as a constant, from earlier arguments, Eq. [8] can be transformed to

$$\text{Rate} = \frac{a[\text{PhCH}_2\text{OH}]}{b + c[\text{PhCH}_2\text{OH}]}. \qquad [9]$$

The model parameters are once again obtained by nonlinear regression and Fig. 5 shows the model fitting. The sum of residuals is 0.998. This result suggests that the two-step Mars–van Krevelen mechanism is most likely occurring in the oxidation of benzyl alcohol over OMS-2.

Oxygen Exchange Reaction

The oxygen isotope experiment gives experimental evidence of the involvement of lattice oxygen in the oxidation mechanism. The qualitative content of the ^{18}O-labeled H_2O formed was determined and the results are shown in Fig. 6. The rate of formation of $H_2{}^{16}O$ and $H_2{}^{18}O$ is the same initially. Since gas-phase oxygen is only $^{18}O_2$, this implies that ^{16}O from the lattice, which was not replaced, is participating in the reaction. This clearly denotes a Mars–van Krevelen mechanism. Studies on these types of nonstoichiometric MnO_x materials show that the presence of

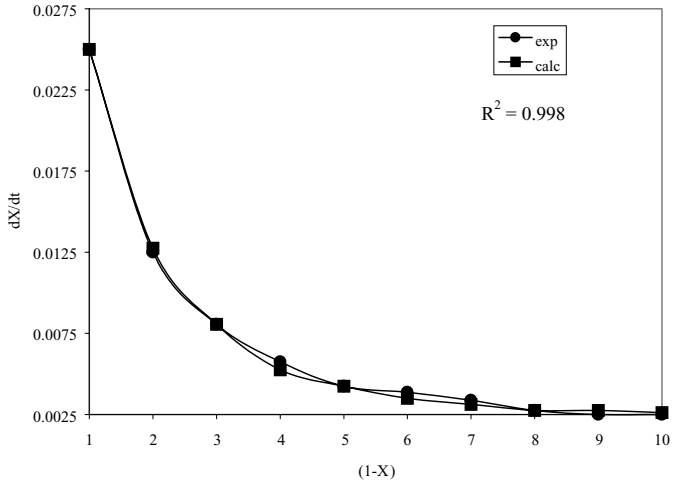

FIG. 5. Mars–van Krevelen kinetic model fitting.

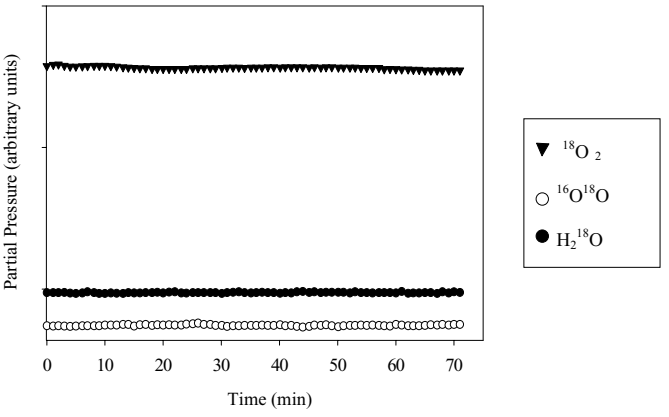

FIG. 7. Physical isotope exchange (scrambling).

intimately coupled Mn^{4+}/Mn^{2+} sites allows electron exchange and, hence, oxygen mobility throughout the surface and the bulk (16–18). The exchange of surface oxygen with its surrounding environment is also easier. As oxygen transport from the surface to the bulk is fast, the surface and bulk oxygen species are indiscernible. Since the catalyst is used in a limiting quantity, as time proceeds, all the ^{16}O in the lattice is used up and replenished by ^{18}O from the gas phase, and further reaction cycles should only produce $H_2{}^{18}O$. This is seen in the latter part of Fig. 6, where the rate of production of $H_2{}^{16}O$ drops off and that of $H_2{}^{18}O$ increases rapidly.

The possibility of oxygen exchange between gas phase and the solid catalyst without the involvement of a redox mechanism needs to be investigated for the above inference to be considered true (19). A scrambling experiment was done, the results of which are shown in Fig. 7. A stream of $^{18}O_2$ was passed over the catalyst in the absence of the substrate to prevent redox reactions from occurring. The catalyst was maintained at the reaction temperature. The exhaust stream was analyzed for $H_2{}^{18}O$ that might be formed by exchange with the structural $H_2{}^{16}O$. As seen from Fig. 7, there is no consumption of $^{18}O_2$ as well as no $H_2{}^{18}O$ formed at 110°C. Also no $^{16}O_2$ or $^{16}O^{18}O$ species were observed from exchange with the lattice oxygen. This validates the interpretation of the isotope-labeling experiment.

Kinetic Isotope Effect

Under the pseudo-first-order rate conditions employed for this experiment, the integrated form of the rate equation is as follows in Eq. 7:

$$\ln\left[\frac{[PhCH_2OH]_o}{[PhCH_2OH]_t}\right] = k_H \cdot t, \qquad [10]$$

where $[PhCH_2OH]_o$ is the initial concentration of benzyl alcohol and $[PhCH_2OH]_t$ is the concentration of benzyl alcohol at time t.

As shown in Fig. 8, a plot of $\ln([PhCH_2OH]_o/[PhCH_2OH]_t)$ vs time gives a straight line whose slope is

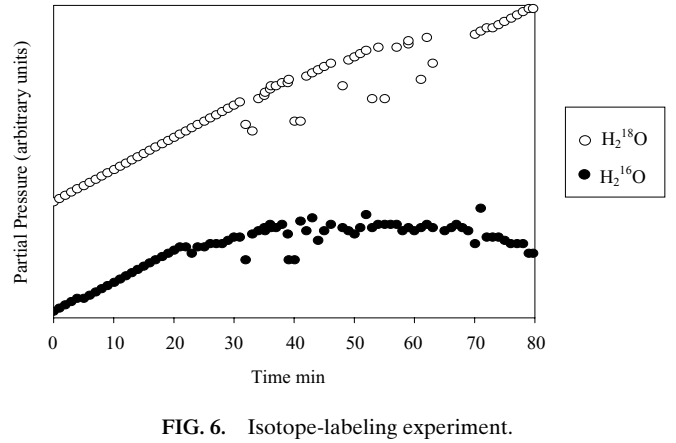

FIG. 6. Isotope-labeling experiment.

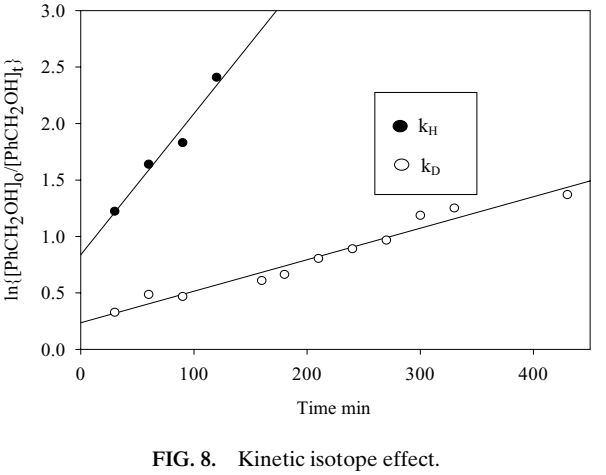

FIG. 8. Kinetic isotope effect.

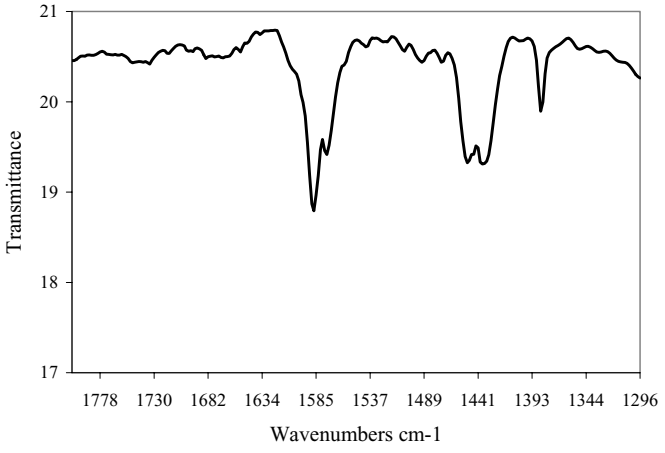

FIG. 9. Acidity measurement of catalyst.

k_H. A similar exercise with $PhCD_2OH$ concentrations gives the value of k_D. The ratio of k_H/k_D at 383 K is calculated to be 4.06, which establishes the presence of a substantial kinetic isotope effect.

Acidity Measurements

The results of the *in situ* IR experiment following pyridine adsorption are shown in Fig. 9. The intense band at ~1440 cm^{-1}can be assigned to pyridine adsorbed on Lewis acid sites. The absence of a peak around 1550 cm^{-1}indicates the lack of strong Brønsted acid sites. However, the peak at ~1590 cm^{-1} denotes hydrogen-bonded pyridine, which implies very weak Brønsted acidity. Thus the catalyst has a dominant Lewis acidity, most probably associated with the Mn^{4+}/Mn^{2+} couple.

DISCUSSION

Westheimer and Nicolaides (20) and others (21) have proposed the use of kinetic isotope effects for ascertaining whether the oxidative attack on the alcohol molecule is at the secondary hydrogen atom or at the hydroxyl hydrogen atom. The fact that C–H and C–D bonds differ in their zero-point energies is used to make this distinction. The presence of an isotope effect greater than 1 would imply that the benzyl alcohol reacts much faster than its dideuterated analogue.

The presence of a large kinetic isotope effect in the present study implies that the removal of a secondary H atom is indeed the rate-controlling step. A mechanism in which the abstraction of the secondary H atom leads to the formation of a free radical is not feasible, as shown by experiments using quinone as a radical trap. These results point to an electron-deficient carbon center in the intermediate formed in the rate-determining step. Equations [11] and [12] summarize this process:

$$PhCH_2OH + Mn^{4+} \xrightarrow{\text{slow}} Ph\overset{+}{C}HOH + H^+ + Mn^{2+}, \qquad [11]$$

$$Ph-\underset{+}{\overset{H}{\overset{|}{C}}}-\overset{\curvearrowleft}{O}-H \xrightarrow{\text{fast}} PhCHO + H^+. \qquad [12]$$

These two steps together constitute the first half of the Mars–van Krevelen mechanism, where the organic substrate is oxidized and the metal undergoes a two-electron reduction. This is consistent with the acidity measurements which show that the Mn^{4+}-type Lewis acid sites are present in the catalyst.

In the second step, the Mn^{2+} undergoes a two-electron reoxidation by oxygen from the fluid phase. Earlier TPR studies on this catalyst (16) show a much higher susceptibility to reduction, as a reduction of Mn^{4+} is involved. This leads to easy release of oxygen species from the lattice and hence a higher oxidation activity. Oxygen can be exchanged on metal oxide surfaces by three known mechanisms—R^0, R^1, and R^2. Of these, the R^1 and R^2 mechanisms are Mars–van Krevelen-type mechanisms, in which one or two oxygens, respectively, from the gas phase are exchanged with lattice oxygen. The R^0 mechanism is a pseudo-Langmuir–Hinshelwood-type mechanism in which the lattice oxygen is not involved and the exchange takes place between two adsorbed molecules. The oxygen exchange occurs as

$$O_2 + \square + 2e^- \rightarrow \underline{O_2^{2-}}, \qquad [13]$$

$$\underline{O_2^{2-}} \underset{-H^+}{\overset{+H^+}{\rightleftharpoons}} HO_2^- + \square \underset{-H^+}{\overset{+H^+}{\rightleftharpoons}} H_2O_2 + \square, \qquad [14]$$

where □ denotes a lattice vacancy and ▬ denotes within the lattice.

The molecular oxygen undergoes a two-electron reduction to form H_2O_2, which is known to decompose easily in another catalytic cycle over OMS-2 to form water as the final end product (22). The data of Doornkamp *et al.* (23) suggest that much higher temperatures are required to achieve a state of the catalyst such that the R^0 mechanism can prevail. The relatively low temperature employed to

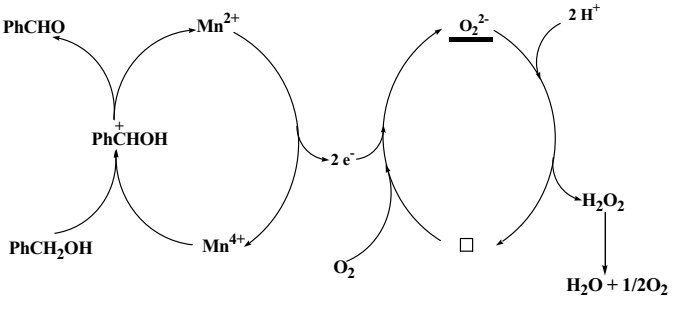

FIG. 10. Overall alcohol oxidation mechanism.

carry out the oxidation (383 K) and the oxygen-labeling experiment conclusively point to a Mars–van Krevelen mechanism. Since an oxygen exchange is involved, the activity of the catalyst would inversely depend on the Mn–O bond strength in the H–K–OMS-2. The high selectivity can also be explained by the same argument. The reaction scheme shown in Fig. 10, incorporating the Mars–van Krevelen-mechanism, can be proposed based on this conclusion.

CONCLUSIONS

K–OMS-2 and its partially acidified form (H–K–OMS-2) were used as catalysts for liquid-phase oxidation of benzyl alcohol in a slurry reactor. The alcohol conversion is >90% after 4 h, with 100% selectivity to aldehyde, making H–K–OMS-2 an excellent catalyst for this reaction. The kinetics of this reaction were investigated and the reaction was found to follow a Mars–van Krevelen-type oxidation mechanism. Not many examples of oxidations are known to occur by this pathway in the liquid phase, due to competition from readily generated free radicals. The proposed mechanism indicates a multielectron redox event occurring in the liquid phase. This result, coupled with the potential of shape selectivity in the regularly ordered tunnels, makes these OMS-2 materials an interesting new class of oxidation catalysts.

ACKNOWLEDGMENTS

We acknowledge support by the Geosciences and Biosciences Division, Office of Basic Energy Sciences, Office of Science, U.S. Department of Energy. We would also like to thank Dr. Francis Galasso for many helpful discussions.

REFERENCES

1. Ley, S. V., and Madin, A., *in* "Comprehensive Organic Synthesis" (B. M. Trost, I. Fleming, and S. V. Ley, Eds.), Vol. 7. p. 251. Pergamon, Oxford, 1991.
2. Choudary, B. M., Kantam, M. L., Rahman, A., Reddy, C. V., and Rao, K. K., *Angew. Chem. Int. Ed. Engl.* **40**(4), 763 (2001).
3. Brink, G. J., Arends, I. W. C. E., and Sheldon, R. A., *Science* **287**, 1636 (2000).
4. Way, Y., DuBois, J. L., Hedman, B., Hodgson, K. O., and Stack, T. D., *Science* **279**, 537 (1998).
5. Skibida, I. P., and Sakharov, A. M., *Catal. Today* **27**, 187 (1996).
6. Mars, P., and van Krevelen, D. W., *Chem. Eng. Sci*. **3** (Special Suppl.), 41 (1954).
7. Arends, I. W. C. E., Sheldon, R. A., Wallau, M., and Schuchardt, U., *Angew. Chem. Int. Ed. Engl*. **36**, 1144 (1997).
8. Doornkamp, C., Clement, M., and Ponec, V., *Appl. Catal. A* **188**, 325 (1999).
9. Abon, M., Bere, K. E., and Delichere, P., *Catal. Today* **33**, 15 (1997).
10. Khemkin, A. M., and Neumann, R., *Angew. Chem. Int. Ed. Engl.* **39**(22), 4088 (2000).
11. Son, Y.-C., Makwana, V. D., Howell, A. R., and Suib, S. L., *Angew. Chem. Int. Ed. Engl.* **40**(22), 4280 (2001); *Angew. Chem.* **113**, 4410 (2001).
12. Shen, Y. F., Zerger, R. P., DeGuzman, R. N., Suib, S. L., McCurdy, L., Potter, D., and O'Young, C. L., *J. Chem. Soc. Chem. Commun.* 1213 (1992).
13. Shen, Y. F., Zerger, R. P., DeGuzman, R. N., Suib, S. L., McCurdy, L., Potter, D., and O'Young, C. L., *Science* **260**, 511 (1993).
14. DeGuzman, R. N., Shen, Y. F., Suib, S. L., Shaw, B. R., and O'Young, C. L., *Chem. Mater*. **5**, 1395 (1993).
15. Fogler, H. S., "Elements of Chemical Reaction Engineering," 3rd ed. Prentice–Hall, Englewood Cliffs, NJ, 1998.
16. Yin, Y. G., Xu, W. Q., DeGuzman, R., Suib, S. L., and O'Young, C. L., *Inorg. Chem.* **33**, 4384 (1994).
17. Yin, Y. G., Xu, W. Q., Shen, Y. F., Suib, S. L., and O'Young, C. L., *Chem. Mater.* **6**, 1803 (1994).
18. Yin, Y. G., Xu, W. Q., Suib, S. L., and O'Young, C. L., *Inorg. Chem.* **34**, 4187 (1995).
19. Chen, K., Iglesia, E., and Bell, A. T., *J. Phys. Chem.* **B105**, 646 (2001).
20. Westheimer, F. H., and Nicolaides, N., *J. Am. Chem. Soc.* **71**, 25 (1949).
21. Goldman, I. M., *J. Org. Chem.* **34**, 3289 (1969).
22. Zhou, H., Shen, Y. F., Wang, J. Y., Chen, X., O'Young, C. L., and Suib, S. L., *J. Catal.* **176**, 321 (1998).
23. Doornkamp, C., Clement, M., and Ponec, V., *J. Catal.* **182**, 390 (1999).